Supporting Information

Hypocrellin-based Multifunctional Phototheranostic Agent for NIR Triggered Targeted Chemo/photodynamic/photothermal Synergistic Therapy against Glioblastoma

Chuangli Zhang[a,b], Jiasheng Wu[a,], Weimin Liu[a,b], Xiuli Zheng[a], Wenjun Zhang[c], Chun-Sing Lee[c] and Pengfei Wang[a,b,*]*

[a] Key Laboratory of Photochemical Conversion and Optoelectronic Materials and CityU-CAS Joint Laboratory of Functional Materials and Devices, Technical Institute of Physics and Chemistry, Chinese Academy of Sciences, Beijing 100190, P. R. China

[b] School of Future Technology, University of Chinese Academy of Sciences, Beijing 100049, P. R. China

[c] Center of Super-Diamond and Advanced Films (COSDAF) & Department of Materials Science and Engineering, City University of Hong Kong, Kowloon 999077, Hong Kong SAR, People's Republic of China

[*]Corresponding authors: wujs@mail.ipc.ac.cn; wangpf@mail.ipc.ac.cn

Table S1. Loading rates of **TMZ-C18** and **DCHB** in the different nanoparticles and corresponding particle size from TEM, DLS and zeta potential analyses.

Nanoparticle	**TMZ-C18** encapsulation (wt %)	**DCHB** encapsulation (wt %)	TEM size	DLS size	Zeta potential
T NPs	15.95 %	N/A	66 nm	89 nm	-32.9 mV
D NPs	N/A	16.21 %	66 nm	90 nm	-32.6 mV
DT NPs	5.80 %	8.36 %	67 nm	94 nm	-32.7 mV
DTRGD NPs	5.83 %	8.41 %	68 nm	95 nm	-24.3 mV

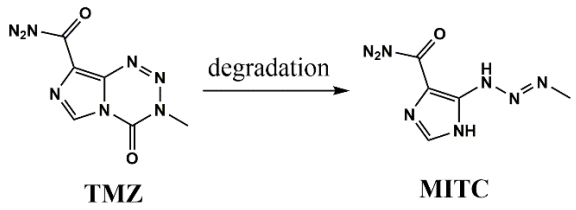

Figure S1. The process of TMZ degradation into MITC.

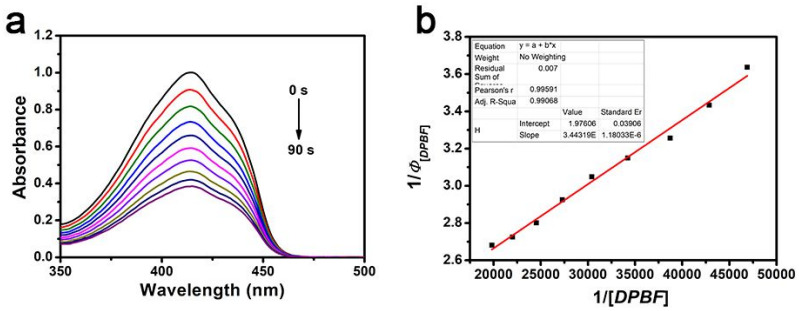

Figure S2. (a) Photodegradation of DPBF with **DCHB** under 721 nm laser irradiation. (b) Linear relationship from decay curves in (a).

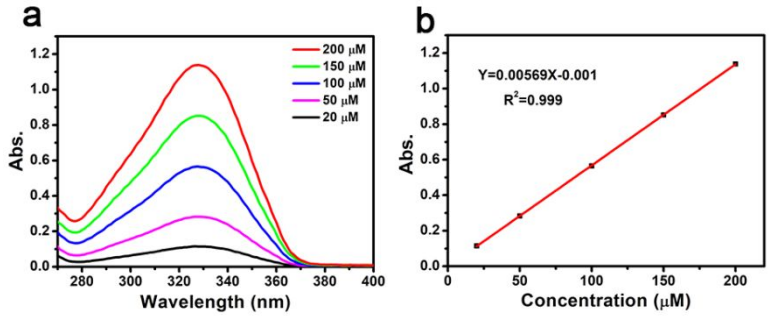

Figure S3. (a) UV-vis absorption spectrum of **TMZ-C18** in DMF with different concentrations. (b) Absorption calibration curve of **TMZ-C18** at 328 nm.

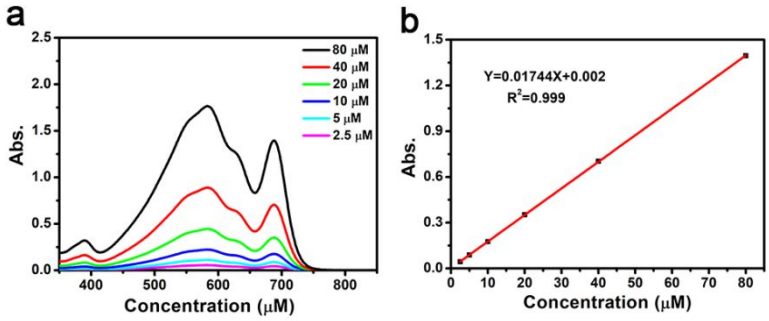

Figure S4. (a) UV-vis absorption spectrum of **DCHB** in DMF with different concentrations. (b) Absorption calibration curve of **DCHB** at 688 nm.

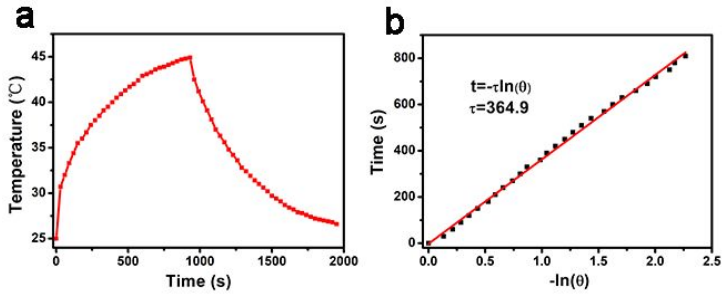

Figure S5. (a) Photothermal effect of **DTRGD NPs** exposed to 721 nm laser irradiation (0.5 W cm^{-2}) for 15 min. (b) Plot of the cooling time (15 min) *vs* the negative natural logarithm of the temperature driving force obtained from the cooling stage in (a).

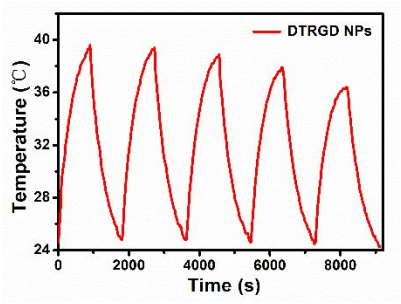

Figure S6. Temperature variations in the solution of **DTRGD NPs** under 721 nm laser irradiation at the power density of 0.5 W cm^{-2} for five cycles.

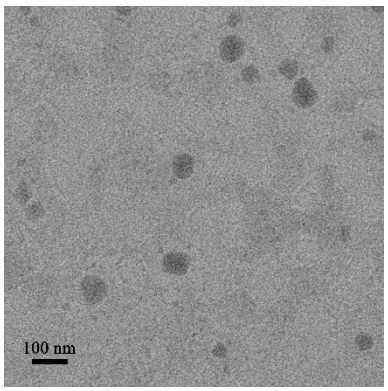

Figure S7. TEM image of **DTRGD NPs** after laser irradiation.

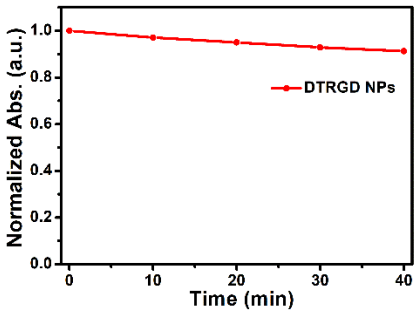

Figure S8. Photostability of **DTRGD NPs** exposed to 721 nm laser irradiation (0.5 W cm^{-2}) for 40 mins.

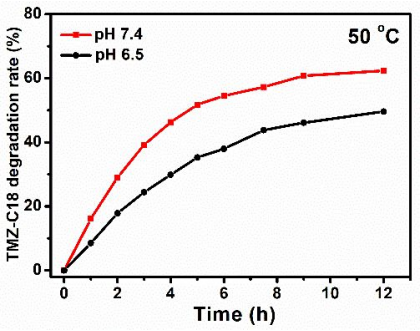

Figure S9. **TMZ-C18** degradation rates in PBS buffer (pH 6.5 or 7.4) at 50 °C.

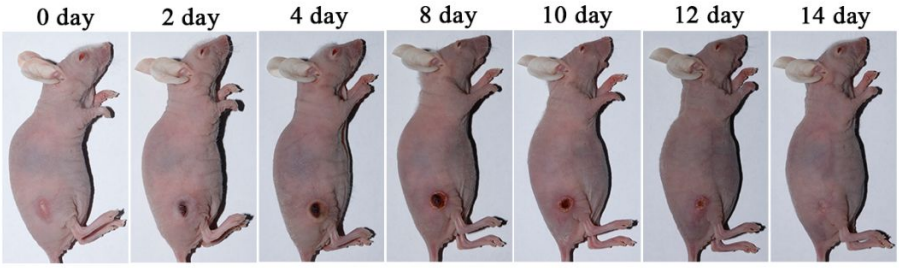

Figure S10. Photographs of the mice in group V with different days after treatment.

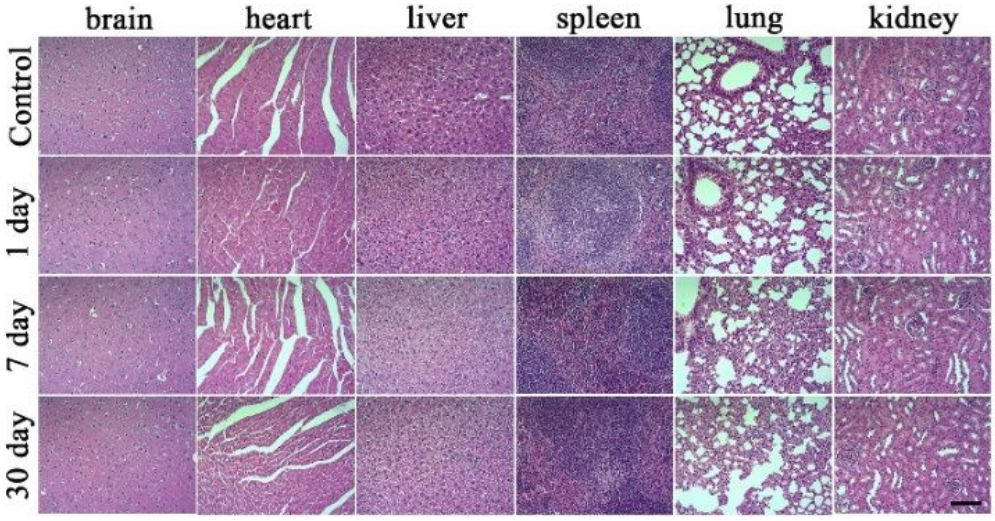

Figure S11. H&E-stained images of the brain, heart, liver, spleen, lung, and kidney in mice on 1, 7, and 30 d post-i.v. injection of **DTRGD NPs**, normal mice served as control. Scale bar: 100 μm.

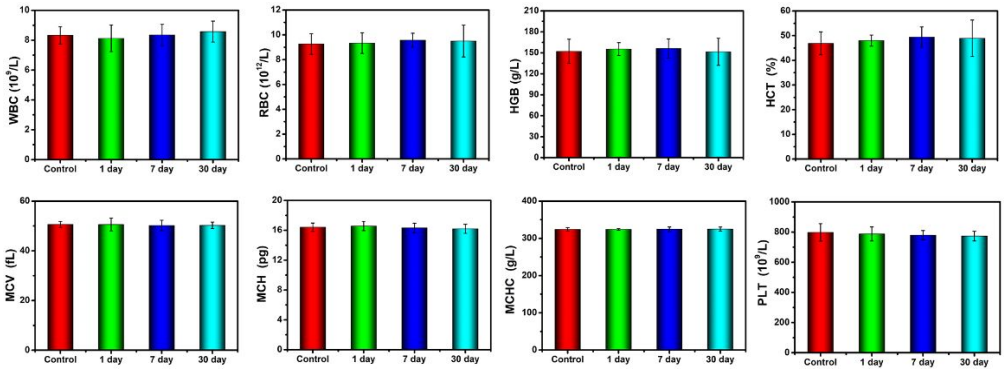

Figure S12. Routine blood tests of mice on 1, 7, and 30 d post-i.v. injection of **DTRGD NPs**, normal mice served as control (n=4). Data note: WBC: white blood cells, RBC: red blood cells, HGB: hemoglobin, HCT: hematocrit, MCV: mean corpuscular volume, MCH: mean corpuscular hemoglobin, MCHC: mean corpuscular hemoglobin concentration, PLT: platelets,

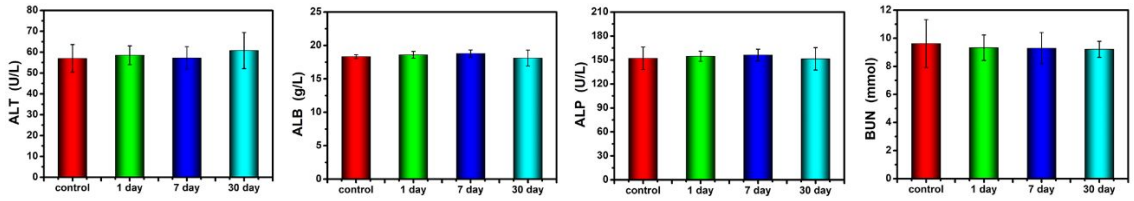

Figure S13. Serum biochemical parameters of mice on 1, 7, and 30 d post-i.v. injection of **DTRGD NPs**, normal mice served as control (n=4). Data note: ALT: alanine aminotransferase, ALB: albumin blood, ALP: alkaline phosphatase urea, BUN: nitrogen.